Photocatalytic degradation of caffeine and *E. coli* inactivation using silver oxide nanoparticles obtained by a facile green co-reduction method

Harshiny Muthukumar (harshiny37@gmail.com)
Indian Institute of Technology Madras
Santosh Kumar Palanirajan
Indian Institute of Technology Madras
Manoj Kumar Shanmugam
Indian Institute of Technology Madras
Arivalagan Pugazhendhi
Ton Duc Thang University
Sathyanarayana N. Gummadi
Indian Institute of Technology Madras

Research Article

Keywords: Silver oxide, Photocatalytic degradation, Caffeine, E. coli, Antibacterial, Inactivation

Posted Date: April 30th, 2021

DOI: https://doi.org/10.21203/rs.3.rs-245921/v1

Version of Record: A version of this preprint was published at Clean Technologies and Environmental Policy on June 11th, 2021. See the published version at https://doi.org/10.1007/s10098-021-02135-7.

Abstract

In this study, silver oxide nanoparticles (Ag_2O-NPs) were synthesized from silver nitrate using green amaranth leaf extract as reducing agent. The degradation of caffeine and inactivation of *Escherichia coli* by Ag_2O-NPs was studied under compact fluorescent lamp illumination irradiation. Apart from that, the antibacterial and antioxidant activities of Ag_2O-NPs were also examined. Synthesized Ag_2O-NPs were shaped like monodispersed husk, and cubic structured with surface area and average particle size was detected to be 100.21 (m^2/g) and 81 nm respectively. Antioxidant efficacy of the Ag_2O-NPs was evaluated using 1, 1-diphenyl-2-picrylhydrazyl and 91% inhibition was achieved with 100 µg Ag_2O-NPs. Bacteriocidic propensity of Ag_2O-NPs was examined against the *S. aureus* and *P. aeruginosa* by disc diffusion, minimum inhibitory concentration (MIC), Live and dead assay. It was observed that the NPs have higher bactericidal effect on Gram-negative as compared to Gram-positive bacteria. Up to 96% photocatalytic inactivation of *E. coli* was achieved using 30 µg/mL of NPs, Photocatalytic degradation of caffeine (50 ppm initial concentration) was observed to be 99% at pH 9 in 15 h using 50 mg/L of Ag_2O NPs. These results indicate that Ag_2O NPs can be employed in environmental applications like harmful bacteria inactivation and organic pollutants degradation.

Introduction

The rising rate of drug-resistance to current antibiotics microbial infections and adverse toxic effects of some antibiotics warranted alternative of new drugs (Wang et al. 2018; Roy et al. 2019). In this regard, nanotechnology is a forthcoming research topic in area of infectious disease treatment with the advancement of nano-scale substances with enhanced antimicrobial activities against multidrug-resistant microbes (Shanmuganathan et al. 2018). Among the nanomaterials, metal nanoparticles (NPs) give the maximum effective outcome. Currently, several NPs for instance Ag, Ag_2O, Au, Cu, CuO, CeO_2, Fe, FeO, TiO_2 and ZnO are synthesized via several methods and have several applications such as applied as antimicrobial and anticancer agents, as catalysts, cosmetic, coatings and in nano-device (Schröfel et al. 2014; Aiswarya Devi et al. 2017; Pugazhendhi et al. 2018). However, the application of NPs was limited in real-time usages, such as clinical, environmental remediation/reclamation, water treatment material, etc., primarily due to the physicochemical properties of NPs such as low solidity, high solubility, monodispersity, wide bandgap, and adverse noxious effect (Kahru and Dubourguier 2010).

It has been reported that nanosized silver particles (size < 100 nm), hold high stability, surface-area-to-volume ratio, have a bandgap of 1.3 eV and are less toxicity (Jiang et al. 2015). Silver nanoparticles been extensively used as antimicrobial and drug delivery agents as well as more efficient photocatalyst under visible light compared to many other metal oxides (Yang et al. 2015). Till date, NPs have been prepared by physical, chemical, electrochemical, sonochemical, irradiation, and biological routes (Iravani, S, Korbekandi, H, Mirmohammadi, SV, Zolfaghari 2014). Use of plant sources in synthesis of nanoparticles offers several advantages from previously documented process since this process is biocompatible, non-toxic, non-hazardous, economical, eco-friendly, and sustainable. Moreover, plant sources satisfy the roles

of stabilizing, reducing, and capping materials (Ahmed et al. 2016; Elemike et al. 2017). The extract of various plants has been used for the biosynthesis of NPs (Siddiqi et al. 2018). Among the plant extracts studied, *aqueous* leaf extracts of Amaranthus. *sp.* hold many organic compounds and have been used for the synthesis of NPs (Muthukumar et al. 2020a).

The choice of microbes in the current study was based on noxious traits toward human health. *Staphylococcus aureus* is a Gram-positive (+ ve), round bacterium which is the causal agent of pulmonary infections and urinary tract infections(Taylor, and Unakal 2019). *Pseudomonas aeruginosa* is a Gram-negative (-ve), rod-shaped bacterium and a multidrug-resistant pathogen implicated in nosocomial infections, external ear canal infection (Pang et al. 2019). It is also imperative to improve characteristics of visible-light-driven bactericidal photocatalysts (Ren et al. 2009; Ganguly et al. 2018). The identification of harmful nano technology and materials used for synthesis of nano particles and also confirming the techniques and materials described as harmless is essential in exploring new applications of nanoparticles (Nel et al. 2010).

Currently, pharmaceuticals and personal care product have gained inattention as emerging micropollutants threats to the marine environment and human health. Among that, Caffeine has been detected in surface water worldwide and being used as a chemical marker for surface water pollution. Also, it is very hard to remove and degrade by conventional treatment methods. It was reported that, the green mediated semiconductors photocatalysis and ability to utilize light source was recognized to be an efficient technology for wastewater treatment [20].

Based on the above considerations, in this study, Ag_2O-NPs have been produced using aqueous leaf extract of green amaranth as a reducing and capping agent. The morphology, composition and structural characteristic of synthesized Ag_2O-NPs were analyzed. Further, antioxidant activity of Ag_2O-NPs was estimated by 2,2-diphenyl-1-picrylhydrazyl (DPPH) assay. Cytotoxicity of the synthesized Ag_2O-NPs was tested against human embryonic kidney (non-cancerous) cells (HEK 293T) by (3-(4,5-dimethylthiazolyl-2)-2,5-diphenyltetrazolium bromide) MTT assay. Antibacterial activity of Ag_2O-NPs was examined against the *S. aureus* and *P. aeruginosa* by disc diffusion, minimum inhibitory concentration (MIC) and Live and dead assay. The photocatalytic inactivation and degradation of *E. coli* and caffeine using leaf extract mediated Ag_2O-NPs under compact fluorescent lamp irradiation were also studied.

Experimental Methods

2.1. Materials

Chemicals such as ascorbic acid, DPPH, dimethyl sulfoxide (DMSO), kanamycin, silver nitrate ($AgNO_3$), nutrient broth, and agar-agar were obtained from Merck and Himedia Laboratories (Mumbai, India). Bacterial strains *E. coli* (MTCC 7410), *P. aeruginosa* (MTCC-2488) and *S. aureus* (MTTC 424) were obtained from the Microbial Type Culture Collection, Chandigarh, India.

2.2. Synthesis of nanoparticles

For synthesis of Ag_2O-NPs, 1 mM silver nitrate ($AgNO_3$) solution and 20 g aqueous leaf extract were used as source of Ag^+ ions and reducing mediator respectively. Leaf extract was prepared as per the previous reported protocol (Muthukumar et al. 2020a). 25 ml of leaf extract solution (pH 6.0) was slowly added to 75 mL $AgNO_3$ solution for 15–20 min at 35± 2 °C under continuous stirring using a magnetic stirrer. Formation of Ag_2O-NPs was indicated by change in color of precursor solution from colorless to brown. The obtained particles were centrifuged at 12,000 rpm for 20 min and washed three times with Milli-Q H_2O followed by drying at 100 ± 2 °C. Finally, the obtained particles were kept in a hermetically sealed bottle for future use.

2.3. Characterization techniques

Crystal structure of Ag_2O-NPs was investigated using a X-ray diffractometer (PANalyticalX'per PRO) equipped with a Cu Kα radiation (I = 1.5406 Å) at 2.2 kW Max. Morphological features of NPs were studied using a scanning electron microscope (SEM Carl Zeiss Evo 18 Germany) and the images were captured at 20 kV. Fourier transform infrared spectroscopy (FTIR) analysis of aqueous leaf extract and NPs was carried out at a scan range of 4000–400 cm^{-1} and scanning speed of 2 mm s^{-1} on a IR Pestige-21 instrument (Shimadzu). Size and zeta potential of NPs were evaluated using Malvern Zetasizer (Ver. 7.02, Malvern Instruments Ltd) dynamic light scattering (DLS) technique. Stained LIVE/DEAD bacterial cells were observed under an ECLIPSE 80i fluorescence microscope (Nikon, Japan) with Spot-K slider CCD camera (Diagnostic Instruments Inc., USA).

2.4. Antimicrobial and antioxidant activity

The bactericidal activity of Ag_2O-NPs against *S. aureus* and *P. aeruginosa was tested* via disk diffusion susceptibility and minimum inhibitory concentration method. Also, antioxidant activity of leaf aqueous extract and NPs were confirmed by DPPH assay. Likewise, the NPs MTT cytotoxicity assay against HEK 293T was carried out as per the previously reported protocol (Muthukumar et al. 2020a, b). All the *experiments* were conducted in *triplicate and* statistical significance of the tests was evaluated using software GraphPad Prism (La Jolla, USA).

2.5. Live and dead assay

Live and dead assay was conducted to examine the bactericidal effect of Ag_2O-NPs. For this, 30 µg/mL of Ag_2O-NPs in solution was loaded into test bacterial culture at 10^5 CFU ml^{-1} concentration and incubated at 37 °C for 24 h. The suspension of bacterial cells was centrifuged and the pellet was resuspended in liquid broth medium (1 mL). The cells were incubated for 10 min at 37 °C with 5 mg/mL of acridine orange and 3 mg/mL propidium iodide. This was followed by centrifugation of the incubated cell suspension at 7000 rpm for 7 min at 4 °C. Supernatant was discarded and the unbonded dyes were removed using 1× phosphate-buffered saline at pH 7.4. The cell suspension (~5 µL) was poured on a

glass slide and covered with the coverslip and cellular images were observed under laser confocal microscopy (Nikon AI (P)) (Thiyagarajan et al. 2018).

2.6. Photocatalytic inactivation property of Ag_2O-NPs

The photocatalytic inactivation (PCI) of Ag_2O-NPs was estimated on the deactivation of *E. coli* under compact fluorescent lamp (CFL) illumination at a concentration of 30 µg/mL. *E. coli* culture was prepared by inoculating bacteria in Lysogeny Broth (LB) medium followed by overnight incubation at 37 °C. PCI experiments were conducted in an incubator with CFL illumination of 85 W(4U), 650 mA current, and 50 Hz frequency which was positioned at 15 cm atop the cell suspension. The tests were conducted in Erlenmeyer's flasks for 15 h at 37 ± 1 °C with continuous agitation at 120 rpm. To know the growth kinetics of *E. coli* 0.5 mL culture samples were collected at one-hour interval and optical density of collected samples was measured at 600 nm by UV-Visible spectrometer. For comparison, experiments were also performed under dark and light conditions.

2.7. Photocatalytic degradation

Photocatalytic degradation of caffeine by NPs was studied under CFL irradiation. Caffeine solution (pH-9.0) containing 50 ppm of caffeine was added to 50 mg/L of Ag_2O-NPs and maintained at 37 ± 1 °C for 15 h under CFL. At regular intervals of time, 0.5 mL sample was collected and centrifuged for 15 min at 7000 rpm. The centrifuged samples were filtered using a Millipore syringe and analysed for caffeine using HPLC at the regular time interval as per protocol described earlier (Muthukumar et al. 2020b).

Results And Discussion

3.1. UV–Vis spectroscopic study

The formation of the reduced Ag_2O-NPs (maximum λ), $AgNO_3$, and leaf extract was detected using UV–visible spectrophotometer at 200–700 nm (Fig. 1A). In case of $AgNO_3$ solution a broad absorption band in the wavelength region from 290 nm to 400 nm centred at 320 nm was observed (Fig 1A). UV-Vis spectra of the $AgNO_3$ solution displayed a small peak around 217 nm which could be attributed to Ag+ ions. Similar results were obtained for leaf extract spectra in earlier studies where polyphenol peak around 220 and a broad peak around 250 nm was observed (Palomares et al. 2013). The UV–visible spectra exhibited a distinct peak at 432 nm and it was due to the surface plasmon resonance (SPR) of Ag_2O-NPs and the peak at 278 nm could be due to oxidized polyphenols in NPs (Fig. 1A). Absorption

peak of metal NPs is conquered by the SPR of leaf extract reduced silver ions (Ag^+) to the Ag_2O-NPs (Rokade et al. 2016).

3.2. IR spectral analysis of Ag_2O-NPs

The FTIR spectra of Ag_2O-NPs and green amaranth leaf extract have been given in Fig 1B. The broad peak at 3330 cm^{-1} indicates the existence of (NH) amine and (OH) hydroxyl group stretching of amaranthine and phenolic compounds respectively. Peaks at 1646, 1450, 1320, 1089, and 850 cm^{-1} denote the existence of aldehyde C—H stretch, C-H alkane stretch, N—O (nitro) stretch N—H and carbonyl group C-O, respectively. The detected peaks were mostly ascribed to phyto-compounds of leaf extract. These phytochemicals have been shown to play a vital role in the formation of NPs (Aiswarya Devi et al. 2017). The presence of 1029 cm^{-1} 1373 cm^{-1} and 1601 cm^{-1} peaks indicates C-O, C-H, C-O groups in the molecule. Also, amaranthine and phenolic compounds present on the extract can donate hydroxyl and amines functional groups, so free carboxylic or amino moieties can bind to free Ag surface (Muthukumar and Matheswaran, 2015). FT-IR spectrum of the dried biosynthesized NPs showed peaks at 588 cm^{-1} which can be attributed to the vibration of AgO and thereby confirming presence of silver oxide in the prepared sample (Ravichandran et al. 2016).

3.3. Structural, shape and size analysis

To confirm the structure and crystallinity of the obtained Ag_2O NPs, XRD analysis was used in further analysis. Fig. 1C shows the XRD pattern recorded from the powder sample of Ag_2O. Braggs reflections 2θ peaks were observed at 32.9°, 38.2°, 55.1°, 66.0°, 69.2° which correspond to (111), (200), (220), (311), and (222) planes of Ag_2O respectively. The observed XRD data were matched to the XRD standard data JCPDS file No. 41-1104 and assigned to the planes of the cubic Ag_2O phase (Rokade et al. 2016). The diffractogram showed that synthesized NPs were crystalline cubic structure and the slight modification in intensity could be due to binding of leaf extract biomolecules to the surface of NPs (Muthukumar et al. 2020a). The chemical state of synthesized NPs has been investigated using by XPS analysis. The XPS spectrum of synthesized NPs was observed in Fig 1C, the peaks of C 1s, and O 1s are observed at 284.8 and 529.5 eV. The visible peaks at 368.5 and 374.5 eV can be ascribed to Ag+ of Ag_2O was observed in XPS survey spectra. Also, high resolution scans of Ag XPS spectra depicted the appearance of small Ag^0 peaks at 369 and 375 eV (data not shown). The XPS examination results visibly showed the co-existence of Ag^0 and Ag_2O. Xu et al., reported that solvent free Ag/Ag_2O nanocomposites show high photocatalytic activity and suitable for practical application of water treatment under the visible-light irradiation (Xu et al. 2018).

The morphology of Ag_2O-NPs was examined using SEM as shown in Fig 2A and B. The SEM images show husk shaped NPs, indicating that the polyphenols act not only as a reducing agent but also as a capping agent. EDX elemental mapping of Ag was conducted and has been given in Fig 2C. The EDX analysis of NPs has been given in Fig 2D. The chemical elemental study confirms composition Ag and O.

Additionally, trace amounts of element C was also present in NPs. The characteristic signals for Ag and O were observed at 3, 0.3 and 0.8 KeV respectively.

The Ag_2O-NPs size distribution, NPs surface charge, area, and pore size have been presented in Table 1. It was observed that size distribution of Ag_2O-NPs ranges from 20 to 150 nm. The average particle size distribution of Ag_2O-NPs was found to be 81 nm. Zeta potential of Ag_2O-NPs was detected as a sharp peak at −67.66 mV. This indicated that the NPs surface was negatively charged and value of −67.66 mV specifies the repulsion among the NPs (Skoglund et al. 2017).The surface area and pore size of Ag_2O-NPs were found to be 100.21 m^2/g and 10nm respectively. The results depicted that leaf extract mediated NPs have better physicochemical characteristic. Hence, synthesized NPs can be effectively used for abundant biological and environmental applications.

3.4. Antioxidant and cytotoxicity assay

The antioxidant capacity of Ag_2O-NPs was estimated by DPPH at different concentrations of NPs ranging from 20 to 100 µg/mL (Fig 3). Ascorbic acid was used as standard in this study. It was observed that 61% inhibition of DPPH activity was observed with aqueous leaf extract at concentration of 150 µg. This is attributed to the bioactive molecules in the leaf extract element H specifically donated by OH reactive groups to eliminate free radicals (Sowndhararajan and Kang 2013). Increase in inhibitory activity from 25 to 91 ± 1% was observed for NPs as shown in Fig 3.

Similar findings have been reported in a study by Maheshwaran et al., where *Z. rosea* flower extract mediated Ag_2O-NPs (100 µg/ml) showed 73.8% antioxidant activity thereby confirming the inhibition potential of Ag_2O-NPs against reactive oxygen species (ROS) (Maheshwaran et al. 2020). The increase in free-radical-scavenging activity of green amaranth mediated Ag_2O-NPs with increasing concentration was equivalent to ascorbic acid. Phytoconstituents such as the phenolic group on the surface of Ag_2O-NPs, with their stable radicals probably confer free radical scavenging activity to the Ag_2O-NPs. The small size of Ag_2O-NPs react readily with the free radicals and thus scavenging is rapid (Skiba 2020). Hence, these Ag_2O-NPs have good potential to be used as enhancers in biomedical practices requiring free radical scavenging.

Cell viability assay demonstrated that NPs treated HEK cells showed small reduction in viability (data not shown). HEK cells were viable up to 30 µg of Ag_2O but beyond this concentration viability of HEK cell was greatly decreased, which indicates that in biomedical applications, concentration above 30 µg/mL NPs could be harmful to the non-cancerous cells. Studies by Sukhanova et al., showed that cytotoxicity of NPs depended on chemical and physical properties as well as types of cells used for the toxic study (Sukhanova et al. 2018). Akter et al., reported that Ag-NPs concentrations 5 to 10 µg/mL and sizes from 10 to 100 nm showed high toxicity in *in-vitro* studies. Their study also demonstrated that NPs could be stimulate cytotoxicity by the formation of ROS thereby leading to cell death. Different cell lines also expressed different responses to cytotoxic action of Ag-NPs (Akter et al. 2018).

3.5. Antibacterial activity

The bactericidal efficiency of the synthesized Ag_2O NPs was analyzed using disk diffusion method. The obtained results are shown in Fig. 4 and Table. S1. Ag_2O-NPs zone of inhibition increases with increasing concentration of Ag_2O-NPs and higher concentrations, the zone of inhibition is equivalent to that observed with the standard antibiotic kanamycin. Synthesized NPs showed higher antibacterial activity as compared to leaf extract (Table S1). Also, at concentration above 30 µg NPs exhibited zone of inhibition equivalent to kanamycin. The improved activity of NPs can be attributed to the leaf extract molecules bound to surface NPs which intensely increase the active site of NPs and preventing aggregation of NPs (Iravani et al., 2014). Similarly, MIC results represented that increasing concentration of NPs lead to a decrease in the final bacterial cell concentration. Optimal MIC was determined to be 35 µg/mL and 45 µg/mL of NPs for *P. aeruginosa* and *S. aureus* respectively (Fig S1).

S. aureus, which is a Gram +ve strain, showed less inhibition due to the existence of thick peptidoglycan cell outer surface, that inhibited the Ag_2O-NPs enter into the bacterial cell (Slavin et al. 2017). In contrast, Gram -ve bacteria have a thin peptidoglycan layer, which makes easy for the Ag_2O-NPs to enter the bacterial cell leading to cell death, thereby accounting for the higher inhibition for *P. aeruginosa*, a Gram -ve strain. It has been reported that bactericidal activity depends upon particle nature and the surface composition of test bacterium. Also, it has been found that bactericidal activity was due to the electrostatic interaction between Ag_2O-NPs and the bacteria cell wall. So Ag_2O-NPs exhibit higher inhibition ability against *P. aeruginosa* (Jiménez-Tototzintle et al. 2018).

Micrographic pictures of green color fluorescence revealed viable bacterial cells and red color fluorescence imageries show a non-viable cell (Fig 5). Interaction between bacteria cell and NPs resulted in reduced size and count of the bacterial cell and physical rupture of membrane which was observed in the microscopic studies. Reports state that bacterial cell wall surface holds good -ve charge that can interact with Ag+ ions easily and enter inside the cell (D'Lima et al. 2020). After NPs interact and enter into the bacteria cells, cell death is mediated by enzyme inhibition, proteins deactivation, induce oxidative stress, and imbalanced electrolyte and modifies the expression of gene (Shaikh et al. 2019). The results indicate that NPs hold effective bactericidal propensity for Gram –ve than Gram +ve bacteria. In Gram +ve species, thick peptidoglycan layer as an outer membrane function as a penetrability barricade as well susceptible to NPs(Muthukumar et al. 2017).

3.6. Photocatalytic inactivation of *E. coli*

In this study, a Gram -ve bacteria *E. coli* was used as model bacteria since it is an indicator microorganism for faecal contamination. Photocatalytic inactivation of *E. coli* was carried out in the presence of 30 µg ml^{-1} NPs with and without CFL irradiation and the results are given in Fig 6a. It was observed that highest inactivation of *E. coli* was achieved with 30 µg ml^{-1} of NPs under CFL irradiation within 3h. Similarly, highest inactivation of *E. coli* was achieved with NPs alone but it took a longer duration (> 5h) but no significant deactivation was achieved with light alone (data not shown). During

photocatalytic process, photogenerated electron–holes pairs separation and electrons on the surface of NPs can be trapped ROS that improves photocatalytic disinfection (Mcevoy and Zhang 2014). The ROS disrupt the *E. coli* cell membrane and inhibit the lag phase of bacterial growth. This is followed by attack on DNA structure, proteins and interruption of the replication process leading to cell death (Vietro et al. 2019). Doody et al., found that Ag^+ ion was ~12- and 5-fold toxic to *B. subtilis* and *E. coli*, respectively than the Ag NPs at same concentrations. Therefore, our experiment notion depicted that the dissolved Ag^+ ion of synthesized material is more toxic to bacteria *P. aeruginosa* and *S. aureus.* In addition (undissolved) Ag_2O NPs of equivalent concentrations also show good activity in presence of light (Doody et al. 2016).

3.7. Photocatalytic degradation of caffeine

Degradation of caffeine by photocatalytic process was investigated by HPLC analysis. Photocatalytic degradation efficiency of NPs at initial concentration of 50 mg/L was examined using 50 ppm caffeine at pH 9 for 15 h under CFL irradiance and data is given in Fig. 6B. The NPs under light irradiance brought about ~ 99% degradation of 50 ppm caffeine. It was stated that compared to acidic pH (4.0) and neutral pH (7.0), alkaline pH 9.0 has a good quantity of hydroxyl ions, which improves caffeine degradation. Thus pH 9.0 was preferred for this study. Previously it has been reported that photocatalytic activities of NPs depend on the physiochemical properties of the photocatalyst (Muthukumar et al. 2020b). Rashmi et al. also showed that *Centella asiatica* mediated Ag_2O-NPs led to the creation of charge carriers and yielded better amount of hydroxyl ions to decolorized AO-8 dye (Rashmi et al. 2020). Creditably, in green amaranth leaf extract mediated Ag_2O-NPs, the biomolecules bound to Ag_2O-NPs and acted as stabilizing agents leading to a larger number of active site NPs. This helps photoelectron to react with many NPs and thereby increases the formation of hydroxyl radical ($OH^{\bullet}$) and thus improved degradation. $OH^{\bullet}$ was considered as a virtuous oxidizing agent and changed caffeine to toxic less compound than the original harmful contaminant (Jogannatha et al. 2017).

Numerous studies have shown that several materials like TiO_2 powder, ZnO, $AgFeO_2$, CeO_2, and TiO_2 NPs have been used for degradation of caffeine. Other degradative processes such as photo-Fenton, sonocatalytic, adsorption, photolysis, and photocatalytic method have been employed to degrade the caffeine (Palma et al. 2018; Nur Fadzeelah et al. 2019; Muthukumar et al. 2020b). Amongst the caffeine degradation processes reported earlier, photocatalytic method with NPs using $AgFeO_2$ by facilitated 100% degradation of caffeine at the high concentrations of 50 ppm and 120 ppm caffeine in synthetic wastewater in 15 and 24 h respectively (Muthukumar et al. 2020b). Similar finding was obtained in our study, where Ag_2O-NPs at 50 mg/L concentration brought about 100% degradation of caffeine within 15 h. This highlights the potential of synthesized NPs to be used for degrading harmful organic contaminants by an eco-friendly approach. Possible mechanism of synthesized NPs photocatalytic degradation and inactivation of caffeine and *E. coli* have been shown in Fig. S2.

Conclusions

The green amaranth aqueous leaf extract interceded Ag^0/Ag_2O-NPs were successfully synthesized and the antimicrobial and antioxidant properties were investigated along with studies on photocatalytic inactivation of *E. coli* and degradation of caffeine using these nanoparticles. Analytical techniques confirmed that NPs have husk shape with cubic phase structure, large surface, less aggregation and smaller sizes and these properties made it as a better physicochemical nanomaterial. As well, trace of Ag^0 in the sample has been identified by XPS. Studies on antibacterial aspects showed that synthesized NPs were more effective on Gram -ve than Gram +ve bacteria. Also, antioxidant efficacy of the NPs (100 µg) was equivalent to the ascorbic acid. HPLC investigated the photocatalytic degradation of NPs and it was found that caffeine by 50 mg/L of NPs samples brought about 99% degradation of caffeine at 50 ppm initial concentration. Moreover, NPs under optimized conditions exhibited effective and rapid photocatalytic inactivation of *E. coli*. These results suggest that synthesized NPs photocatalyst prove to be an eco-friendly method for removal of organic contaminants and inactivation of harmful microbes in the environment.

Declarations

The authors declare that they have no known competing financial interests or personal

relationships that could have appeared to influence the work reported in this paper.

Funding

The present study was carried out by the financial supported by SERB-DST under

National Post-Doctoral Fellowship vide SO. No: PDF/2018/000795.

Credit authorship contribution statement

Harshiny Muthukumar: Conceptualization, Methodology, Formal analysis, Investigation,

Validation and Writing-Original draft, review & editing.

Manoj Kumar, P. Santosh Kumar, A. Pugazhendhi – Methodology. review and editing

Sathyanarayana N Gummadi: Conceptualization, Resources, Methodology, Supervision and

Writing-original draft, review and editing.

Acknowledgement

The authors would like to acknowledge IIT Madras for the research facilities. SKP and MKS would like to thank MHRD and IIT Madras for the fellowship. MH acknowledges SERB-DST for the National Post-Doctoral Fellowship (SO. No: PDF/2018/000795). Authors would like to acknowledge SAIF-IIT Madras for

characterization studies. MH thank Dr. Swathi Sucharita Dash for their helpful comments on the manuscript.

References

Ahmed S, Ahmad M, Swami BL, Ikram S (2016) A review on plants extract mediated synthesis of silver nanoparticles for antimicrobial applications: A green expertise. J. Adv. Res. 7:17–28. https://doi.org/10.1016/j.jare.2015.02.007

Aiswarya Devi S, Harshiny M, Udaykumar S, et al (2017) Strategy of metal iron doping and green-mediated ZnO nanoparticles: Dissolubility, antibacterial and cytotoxic traits. Toxicol. Res. 6:854–865. https://doi.org/10.1039/c7tx00093f

Akter M, Sikder T, Rahman M, et al (2018) A systematic review on silver nanoparticles-induced cytotoxicity : Physicochemical properties and perspectives. J. Adv. Res. 9:1–16. https://doi.org/10.1016/j.jare.2017.10.008

D'Lima L, Phadke M, Ashok VD (2020) Biogenic silver and silver oxide hybrid nanoparticles: A potential antimicrobial against multi drug-resistant: *Pseudomonas aeruginosa*. New. J. Chem. 44:4935–4941. https://doi.org/10.1039/c9nj04216d

Doody MA, Wang D, Bais HP, Jin Y (2016) Differential antimicrobial activity of silver nanoparticles to bacteria *Bacillus subtilis* and *Escherichia coli* , and toxicity to crop plant Zea mays and beneficial B . subtilis -inoculated. **J** Nanopart Res. https://doi.org/10.1007/s11051-016-3602-z

Elemike EE, Onwudiwe DC, Ekennia AC, et al (2017) Green synthesis of Ag/Ag_2O nanoparticles using aqueous leaf extract of *Eupatorium odoratum* and its antimicrobial and mosquito larvicidal activities. Molecules 22:1–15. https://doi.org/10.3390/molecules22050674

Ganguly P, Byrne C, Breen A, Pillai SC (2018) Antimicrobial activity of photocatalysts: Fundamentals, mechanisms, kinetics and recent advances. Appl. Catal. B-Environ 225:51–75. https://doi.org/10.1016/j.apcatb.2017.11.018

Iravani, S, Korbekandi, H, Mirmohammadi, SV, Zolfaghari B (2014) Synthesis of silver nanoparticles: chemical, physical and biological methods. Res Pharm Sci 9:385–406

Jiang W, Wang X, Wu Z, et al (2015) Silver oxide as superb and stable photocatalyst under visible and near-infrared light irradiation and its photocatalytic mechanism. Ind. Eng. Chem. Res 54:832–841. https://doi.org/10.1021/ie503241k

Jiménez-Tototzintle M, Ferreira IJ, da Silva Duque S, et al (2018) Removal of contaminants of emerging concern (CECs) and antibiotic resistant bacteria in urban wastewater using UVA/TiO2/H2O2 photocatalysis. Chemosphere 210:449–457. https://doi.org/10.1016/j.chemosphere.2018.07.036

Jogannatha RB, Ramu SR, Padaki M, Balakrishna RG (2017) An efficient method for the synthesis of photo catalytically active ZnO nanoparticles by a gel-combustion method for the photo- degradation of Caffeine. Nanochem Res 2:1–10. https://doi.org/10.22036/ncr.2017.01.008

Kahru A, Dubourguier HC (2010) From ecotoxicology to nanoecotoxicology. Toxicology 269:105–119. https://doi.org/10.1016/j.tox.2009.08.016

Maheshwaran G, Nivedhitha Bharathi A, Malai Selvi M, et al (2020) Green synthesis of Silver oxide nanoparticles using *Zephyranthes Rosea* flower extract and evaluation of biological activities. J. Environ. Chem. Eng. 8:104137. https://doi.org/10.1016/j.jece.2020.104137

Mcevoy JG, Zhang Z (2014) Antimicrobial and photocatalytic disinfection mechanisms in silver-modified photocatalysts under dark and light conditions. J. Photochem. Photobiol. C" 19:62–75. https://doi.org/10.1016/j.jphotochemrev.2014.01.001

Muthukumar H, Chandrasekaran NI, Naina Mohammed S, et al (2017) Iron oxide nano-material: physicochemical traits and in vitro antibacterial propensity against multidrug resistant bacteria. J Ind Eng Chem 45:121–130. https://doi.org/10.1016/j.jiec.2016.09.014

Muthukumar H, Matheswaran M (2015) *Amaranthus spinosus* leaf extract mediated feo nanoparticles: physicochemical traits, photocatalytic and antioxidant activity. ACS Sustain Chem Eng. 3:3149–3156. https://doi.org/10.1021/acssuschemeng.5b00722

Muthukumar H, Palanirajan SK, Shanmugam MK, Gummadi SN (2020a) Plant extract mediated synthesis enhanced the functional properties of silver ferrite nanoparticles over chemical mediated synthesis. **Biotechnol Rep.** 26:e00469. https://doi.org/10.1016/j.btre.2020.e00469

Muthukumar H, Shanmugam MK, Gummadi SN (2020b) Caffeine degradation in synthetic coffee wastewater using silverferrite nanoparticles fabricated via green route using *Amaranthus blitum* leaf aqueous extract. J Water Process Eng. 36:101382. https://doi.org/10.1016/j.jwpe.2020.101382

Nel AE, George S, Pokhrel S, et al (2010) Use of a Rapid Cytotoxicity Screening Approach To Engineer a Safer Zinc Oxide Nanoparticle through Iron Doping. Acs Nano 4:15–29. https://doi.org/Doi 10.1021/Nn901503q

Nur Fadzeelah AK, Abdullah AZ, Zubir NA, et al (2019) Sonocatalytic degradation of caffeine using CeO_2 catalyst: Parametric and reusability studies. J. Phys. Conf. Ser 1349:. https://doi.org/10.1088/1742-6596/1349/1/012147

Palma D, Prevot AB, Brigante M, et al (2018) New insights on the photodegradation of caffeine in the presence of bio-based substances-magnetic iron oxide hybrid nanomaterials. Materials 11:1–17. https://doi.org/10.3390/ma11071084

Palomares RI, Navarro RE, Urbina RH, et al (2013) León, E. R., Tánori, J., and Synthesis of silver nanoparticles using reducing agents obtained from natural sources (*Rumex hymenosepalus* extracts). Nanoscale. Res. Lett. . 8 SRC-G:318–326

Pang Z, Raudonis R, Glick BR, et al (2019) Antibiotic resistance in *Pseudomonas aeruginosa*: mechanisms and alternative therapeutic strategies. Biotechnol. Adv. 37:177–192. https://doi.org/10.1016/j.biotechadv.2018.11.013

Pugazhendhi A, Prabakar D, Jacob JM, et al (2018) Synthesis and characterization of silver nanoparticles using *Gelidium amansii* and its antimicrobial property against various pathogenic bacteria. Microb. Pathog. 114:41–45. https://doi.org/10.1016/j.micpath.2017.11.013

Rashmi BN, Harlapur SF, Avinash B, et al (2020) Facile green synthesis of silver oxide nanoparticles and their electrochemical , photocatalytic and biological studies. Inorg. Chem. Commun. 111:107580. https://doi.org/10.1016/j.inoche.2019.107580

Ravichandran S, Paluri V, Kumar G, et al (2016) A novel approach for the biosynthesis of silver oxide nanoparticles using aqueous leaf extract of *Callistemon lanceolatus* (Myrtaceae) and their therapeutic potential. J.Exp. Nanosci. 11:445–458. https://doi.org/10.1080/17458080.2015.1077534

Ren J, Wang W, Zhang L, et al (2009) Photocatalytic inactivation of bacteria by photocatalyst Bi2WO_6 under visible light. Catal. Commun. 10:1940–1943. https://doi.org/10.1016/j.catcom.2009.07.006

Rokade AA, Patil MP, Yoo S Il, et al (2016) Pure green chemical approach for synthesis of Ag_2O nanoparticles. Green Chem Lett Rev s 9:216–222. https://doi.org/10.1080/17518253.2016.1234005

Roy A, Bulut O, Some S, et al (2019) Green synthesis of silver nanoparticles: Biomolecule-nanoparticle organizations targeting antimicrobial activity. RSC Advances 9:2673–2702. https://doi.org/10.1039/c8ra08982e

Schröfel A, Kratošová G, Šafařík I, et al (2014) Applications of biosynthesized metallic nanoparticles - A review. Acta Biomaterialia 10:4023–4042. https://doi.org/10.1016/j.actbio.2014.05.022

Shaikh S, Nazam N, Rizvi SMD, et al (2019) Mechanistic insights into the antimicrobial actions of metallic nanoparticles and their implications for multidrug resistance. Int. J. Mol. Sci. 20:1–15. https://doi.org/10.3390/ijms20102468

Shanmuganathan R, MubarakAli D, Prabakar D, et al (2018) An enhancement of antimicrobial efficacy of biogenic and ceftriaxone-conjugated silver nanoparticles: green approach. Environ. Sci. Pollut. Res. 25:10362–10370. https://doi.org/10.1007/s11356-017-9367-9

Siddiqi KS, Husen A, Rao RAK (2018) A review on biosynthesis of silver nanoparticles and their biocidal properties. J. Nanobiotechnology, 16:. https://doi.org/10.1186/s12951-018-0334-5

Skiba VVGVM (2020) Eco - friendly “ green ” synthesis of silver nanoparticles with the black currant pomace extract and its antibacterial , electrochemical , and antioxidant activity. Appl. Nanosci. https://doi.org/10.1007/s13204-020-01369-z

Skoglund S, Blomberg E, Wallinder IO, et al (2017) A novel explanation for the enhanced colloidal stability of silver nanoparticles in the presence of an oppositely charged surfactant. Phys. Chem. Chem. Phys. 19:28037–28043. https://doi.org/10.1039/c7cp04662f

Slavin YN, Asnis J, Häfeli UO, Bach H (2017) Metal nanoparticles: Understanding the mechanisms behind antibacterial activity. J. Nanobiotechnology. 15:1–20. https://doi.org/10.1186/s12951-017-0308-z

Sowndhararajan K, Kang SC (2013) Free radical scavenging activity from different extracts of leaves of *Bauhinia vahlii* Wight & Arn. Saudi J. Biol. Sci. 20:319–325. https://doi.org/10.1016/j.sjbs.2012.12.005

Sukhanova A, Bozrova S, Sokolov P, et al (2018) Dependence of Nanoparticle Toxicity on Their Physical and Chemical Properties. Nanoscale Res. Lett. 13:. https://doi.org/10.1186/s11671-018-2457-x

Taylor, TA, Unakal C (2019) *Staphylococcus Aureus*. In: Taylor TA, Unakal CG

Thiyagarajan K, Bharti VK, Tyagi S, et al (2018) Synthesis of non-toxic, biocompatible, and colloidal stable silver nanoparticle using egg-white protein as capping and reducing agents for sustainable antibacterial application. RSC Adv. 8:23213–23229. https://doi.org/10.1039/C8RA03649G

Vietro N De, Tursi A, Beneduci A (2019) Photocatalytic inactivation of *Escherichia coli* bacteria in water using low pressure plasma. **Photochem. Photobiol. Sci.18:** 2248-2258. https://doi.org/10.1039/c9pp00050j

Wang W, Arshad MI, Khurshid M, et al (2018) Antibiotic resistance : a rundown of a global crisis. Infect. Drug. Resist. 1645–1658

Xu H, Xie J, Jia W, et al (2018) The formation of visible light-driven Ag / Ag_2O photocatalyst with excellent property of photocatalytic activity and photocorrosion inhibition. J Colloid Interf Sci. 516:511–521. https://doi.org/10.1016/j.jcis.2018.01.071

Yang ZH, Ho CH, Lee S (2015) Plasma-induced formation of flower-like Ag_2O nanostructures. Appl. Surf. Sci. 349:609–614. https://doi.org/10.1016/j.apsusc.2015.05.055

Table

Table 1. Zeta potential, particle size and surface area, pore size of Ag_2O NPs.

NPs	Zeta potential (mV)	Particle size (nm)	Surface area (m^2/g)	Pore size (nm)	Structure
Ag_2O	−67.66	81	100.21	10	cubic

Figures

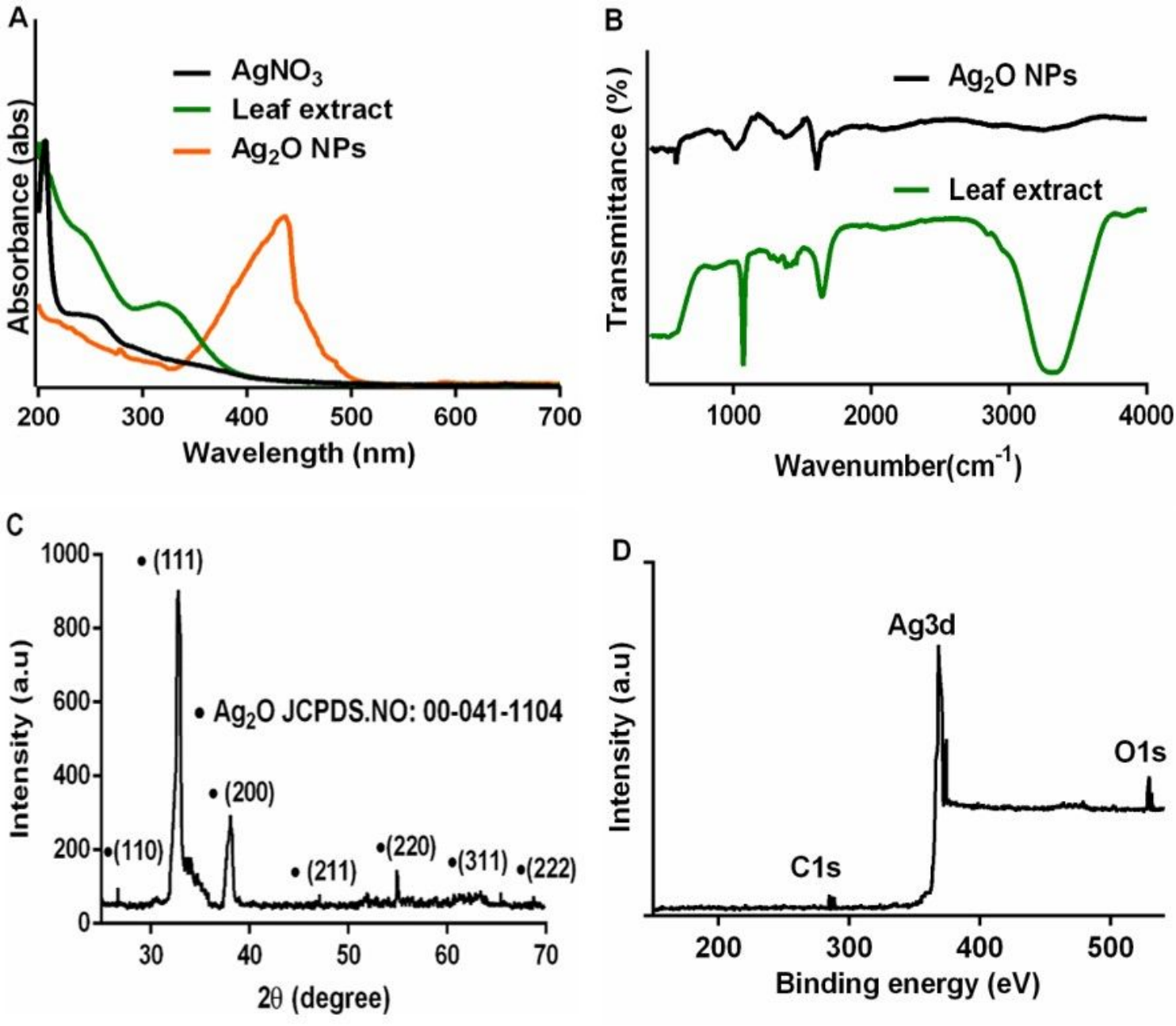

Figure 1

Spectral analysis of green amaranth aqueous leaf extract, AgNO3, Ag2O NPs. (A) Comparison of precursor and Ag2O NPs UV-Vis analysis. The samples were scanned from 200 nm to 900 nm in 1.00 cm path length cuvettes. (B) FTIR spectral analysis of leaf extract and Ag2O NPs obtained over the range of 400 - 4000 cm-1 with a resolution of 4 cm−1 at room temperature. (C) XRD pattern of Ag2O NPs and Diffractogram of NPs also corresponded to JCPDS card no:00-041-1104 AgFeO2. (D) XPS survey spectrum of Ag2O NPs

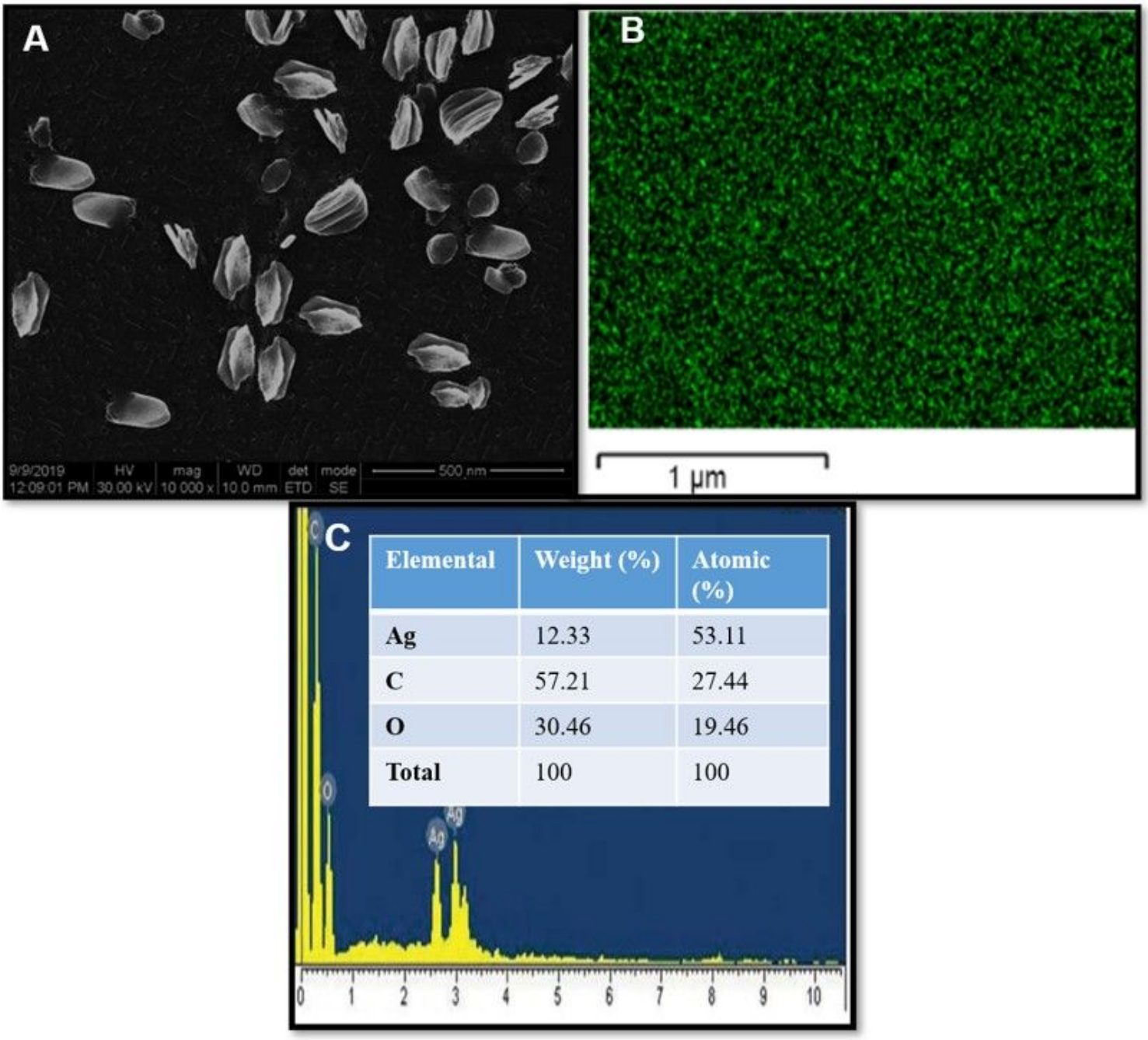

Figure 2

Scanning electron micrograph of synthesized NPs (A, B) SEM images of Ag2O NPs at 500 and 50 nm resolution respectively, EDX elemental analysis (C) Ag element mapping image and SEM operating at a voltage of 30 keV (D) corresponding energy dispersive X-ray spectra of NPs.

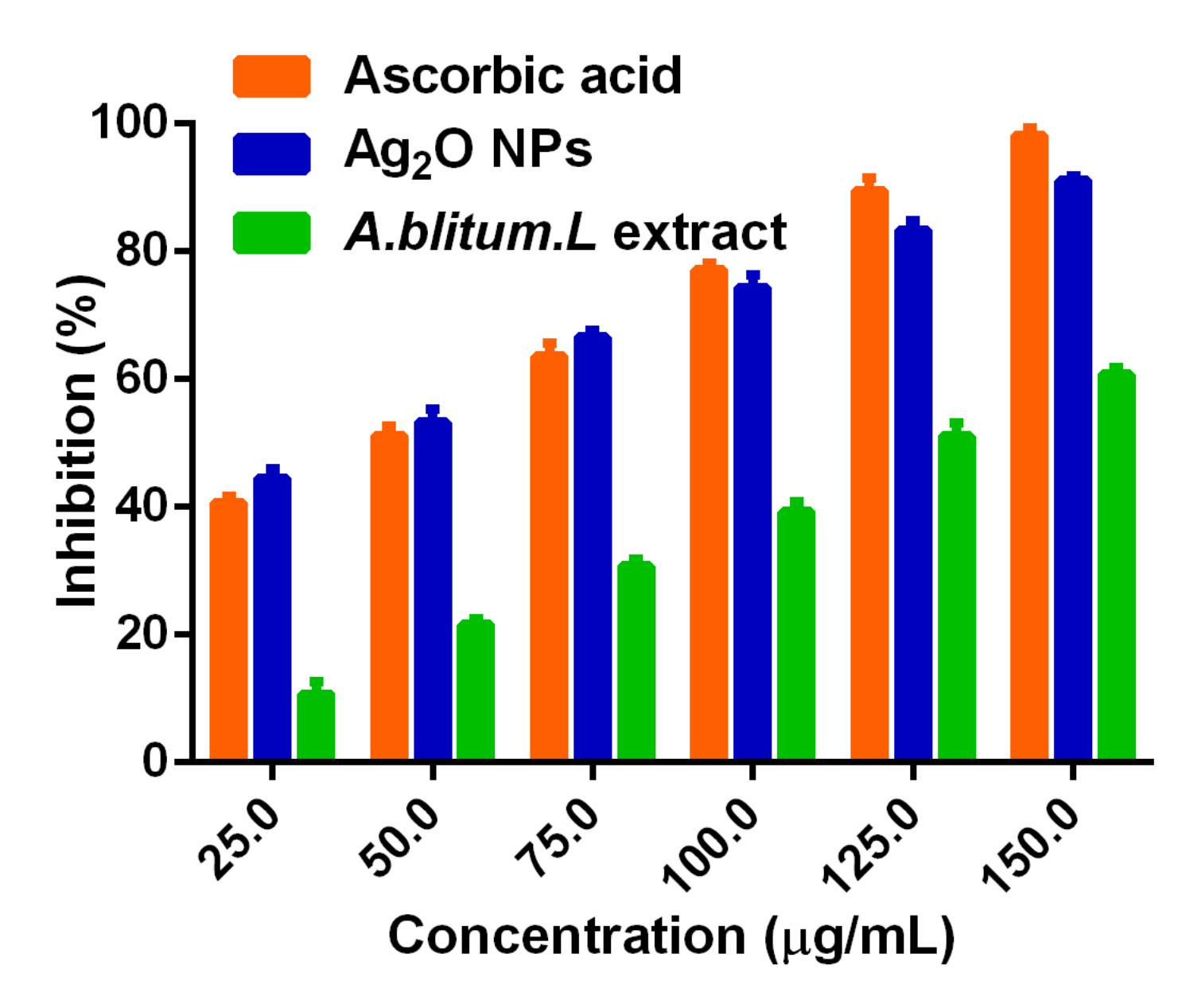

Figure 3

Antioxidant activity by DPPH radical scavenging assay. DPPH scavenging activity of Ag2O NPs compared with the standard ascorbic acid and prepared leaf extract. Results are representative of three replicates and error bars represent standard deviation. One-way ANOVAs were performed to evaluate significance comparing the both NPs to the control. A value of $p < 0.0001$ was considered to be statistically significant as compared to the control.

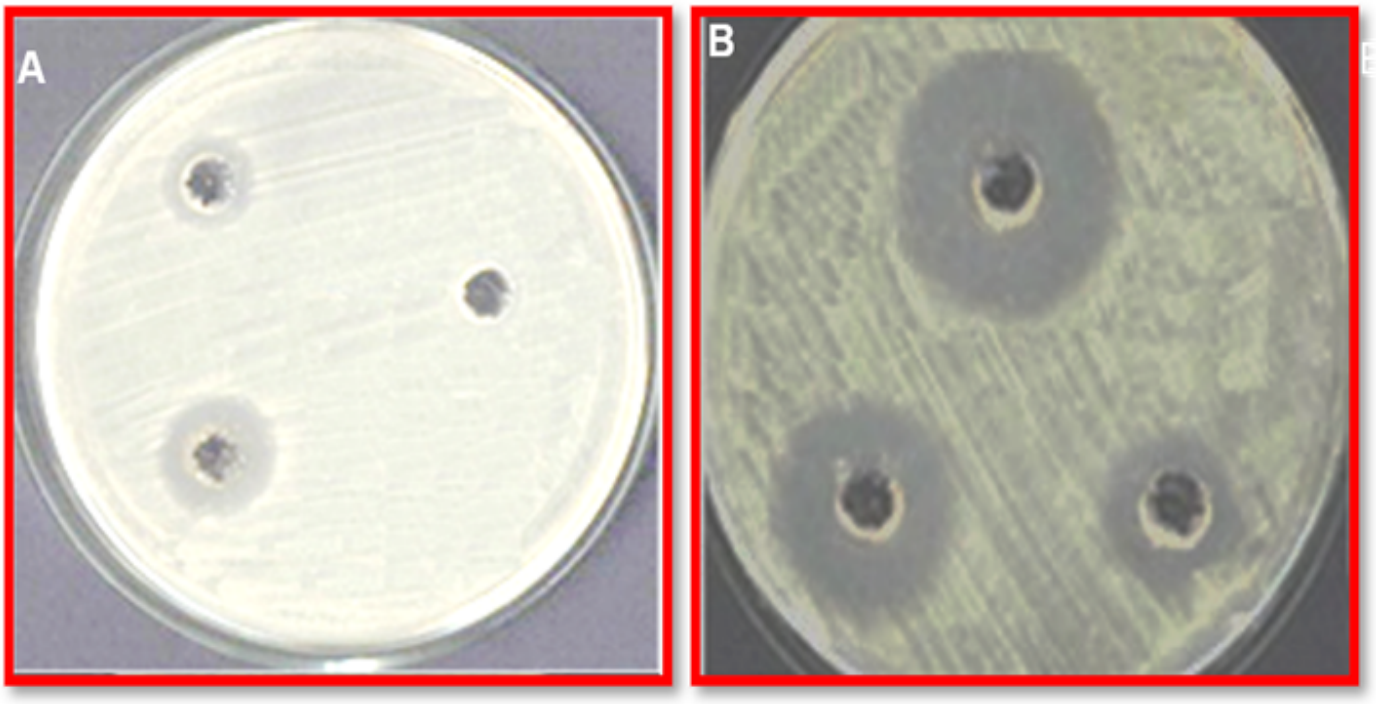

Figure 4

Zone of inhibition (mm) against (A) Staphylococcus aureus and (B) Pseudomonas aeruginosa by disc diffusion and various concentration (10,20 and 30 µg) of NPs.

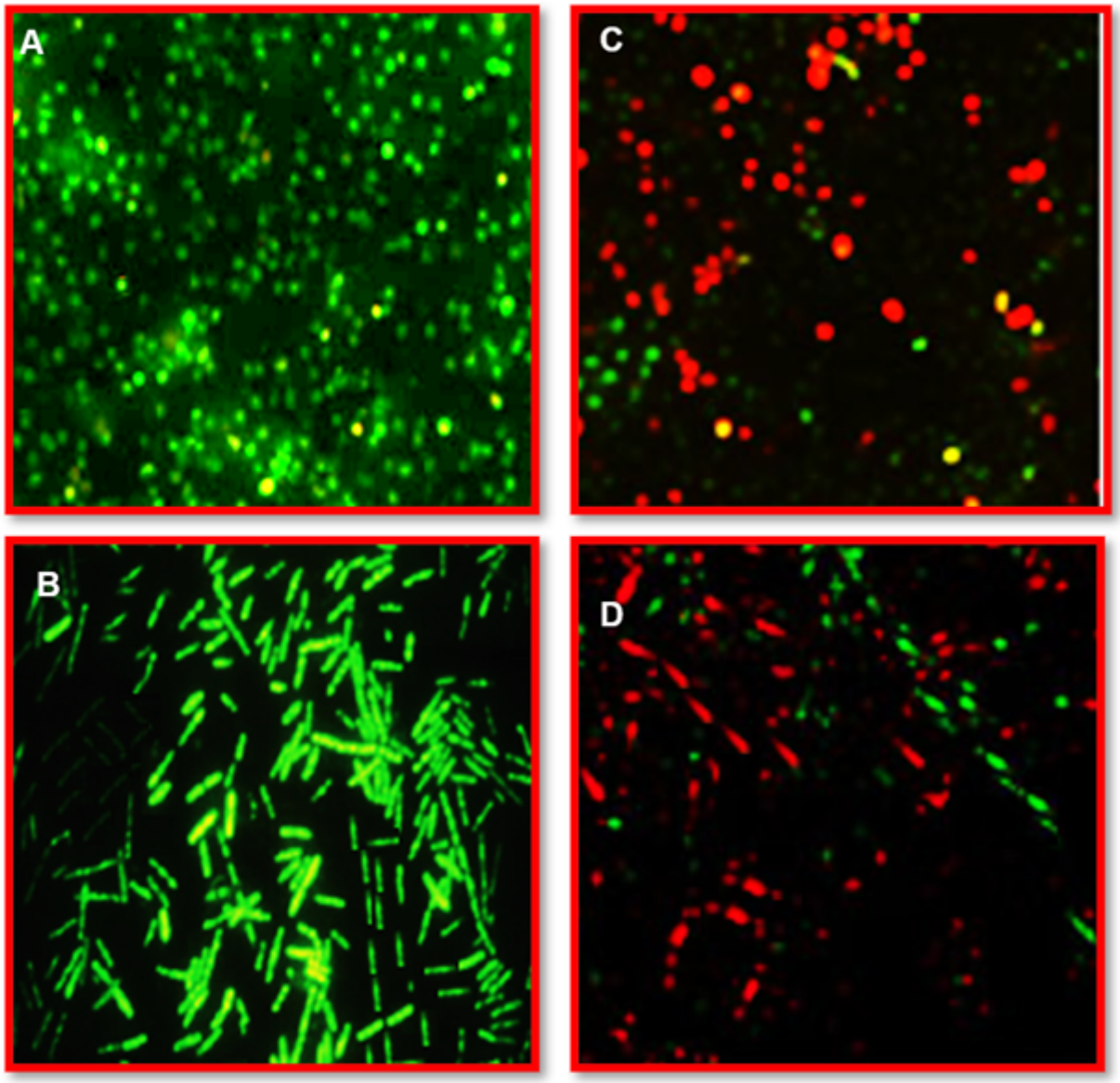

Figure 5

Live/ dead staining of S. aureus and P. aeruginosa exposed to NPs, (A, B) Non-treated test species S. aureus and P. aeruginosa, (C, D) test species S. aureus and P. aeruginosa were exposed to Ag2O NPs microscopic images at magnification of 5 µm.

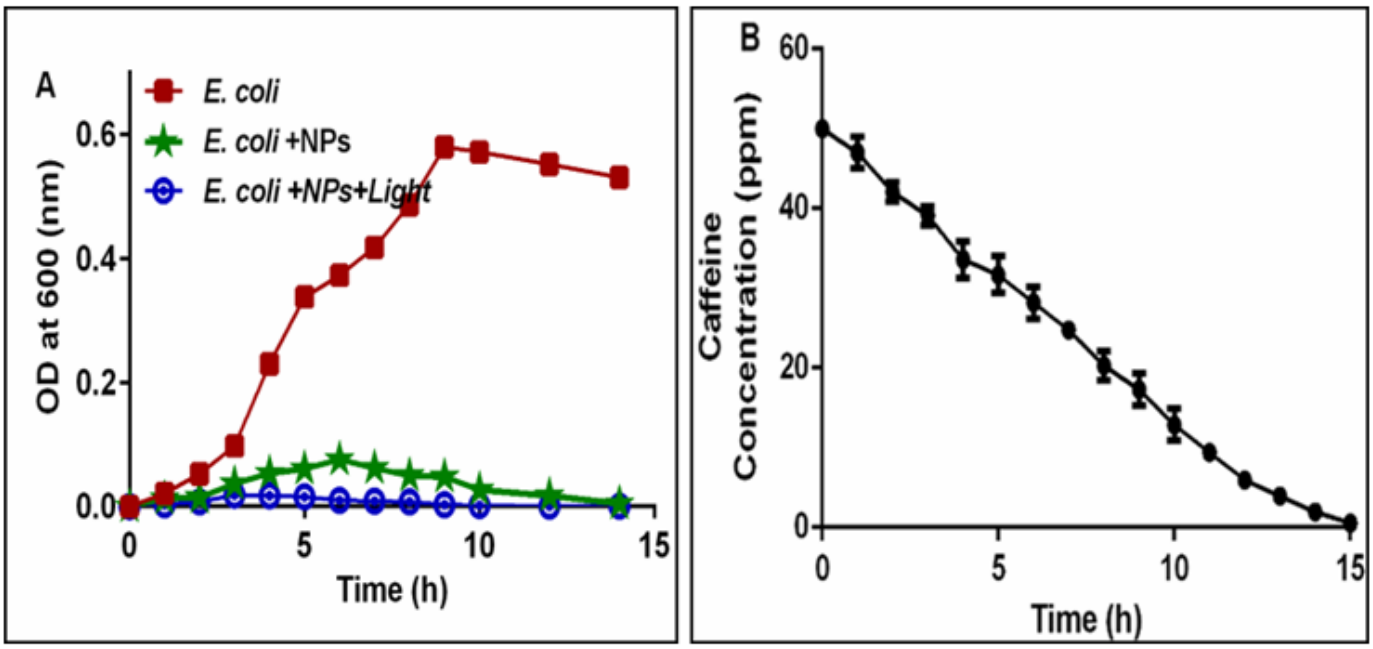

Figure 6

Photocatalytic inactivation of E. coli and photocatalytic degradation of caffeine. (A) E. coli control growth curve and inactivation by synthesised NPs under light and dark condition. (B) The degradation n efficiency of Ag2O NPs on 50 ppm caffeine at pH9 under compact fluorescent lamp illumination condition in the presence of 50 mg/L.

Supplementary Files

This is a list of supplementary files associated with this preprint. Click to download.

- GraphicalabstractsilveroxideJHM.docx
- SupplementraysilveroxideJHM.docx